Limnol. Oceanogr., 46(3), 2001, 679–688

Mesoscale variability of physical and biological fields in southeastern Lake Superior

Meng Zhou,[1] *Yiwu Zhu, Shawn Putnam, and Jay Peterson*
Large Lakes Observatory, University of Minnesota, Duluth, Minnesota 55812

Abstract

A cruise was conducted in southeastern Lake Superior east of Marquette, Michigan from 15 to 20 July 1999. A towed, vertically undulating instrument package containing a conductivity-temperature-depth (CTD) profiler, a fluorometer, and an optical plankton counter was used for data collection. Results indicated that the concurrent, high-resolution survey of both physical and biological variables provided the fundamental basis for illustrating the correlation between mesoscale physical and biological fields and for investigating mesoscale physical and biological processes. It was revealed that the high chlorophyll *a* biomass beneath the thermocline co-occurs with up-tilting of the thermocline. This tilting of the thermocline was associated with the thermally driven coastal current. We hypothesize that the up-tilting of the thermocline lifted deep water into the euphotic zone, leading to high productivity of phytoplankton beneath the thermocline. The presence of both warm water and food provided a favorable physical and biological environment for zooplankton. The abundance of zooplankton reached 10×10^3 individuals m^{-3} in the warm surface water and was down to 3×10^3 individuals m^{-3} at a depth of 40 m.

Lake Superior is the largest freshwater body in North America and has been historically classified as an ultraoligotrophic lake (Matheson and Munawar 1978; Munawar and Munawar 1978). Early studies of biochemical processes suggested that the phytoplankton productivity is limited by nutrients, in particular by phosphate (Weiler 1978; Nalewajko and Lee 1981; Fahnenstiel et al. 1990). Statistical analysis of 144 phytoplankton and zooplankton samples from six cruises in 1971 indicated that the differences between cruises were more pronounced than differences between stations (El-Shaarawi and Munawar 1978; Munawar and Munawar 1978). The spatial distributions of biomass showed homogeneous distribution patterns, but data from both historic and recent studies in Lake Superior showed unexpectedly high zooplankton abundance associated with small and mesoscale physical processes (Olson 1969; Swain et al. 1970; Megard et al. 1997), conflicting with the view of the lake as oligotrophic.

Limited efforts have been made to study mesoscale zooplankton abundance in Lake Superior. A study of zooplankton spatial distribution from 1967 to 1969 by towing two Hardy plankton recorders indicated that the mean zooplankton abundance was relatively low in Lake Superior, but the distribution was very patchy (Olson 1969; Swain et al. 1970). The vertically averaged mean zooplankton abundance was found to be between 10^2 and 10^3 individuals m^{-3} throughout most of the lake (Watson and Wilson 1978). Within a zooplankton patch, the abundance reached $\sim 10 \times 10^3$ individuals m^{-3} (Patalas 1972). This value is equivalent to that of the California Current region (Huntley et al. 1995), which has been regarded as one of the areas with the highest abundance of oceanic zooplankton. Recent acoustic measurements of Lake Superior revealed local patches within which zooplankton abundance reached $5–10 \times 10^3$ individuals m^{-3} and were verified by net samples (Megard et al. 1997).

Much of our thinking about Lake Superior has been driven by lakewide processes. Because the amount of organic material imported into Lake Superior from terrestrial sources is negligible, phytoplankton production primarily supports the whole lake ecosystem (Munawar et al. 1978). Limitations on primary productivity can come from microbial interactions and grazing as well as temperature, amount of light in winter, and nutrient depletion due to the onset of a thermocline in the summer (Weiler 1978). Other evidence has shown that primary productivity and zooplankton patches respond directly to upwelling events induced by wind (El-Shaarawi and Munawar 1978; Lam 1978; Weiler 1978; Megard et al. 1997; Rose and Axler 1998). The northwest shore is a major upwelling area in Lake Superior during the summer. Upwelling events occur once or twice each month in summer and usually persist 2–6 d after windstorms. Such wind-induced upwelling events in Lake Superior were clearly demonstrated in observations and modeling of chloride transports (Lam 1978) and zooplankton distributions (Megard et al. 1997). The recent modeling studies by Chen et al. (2000) and Zhu et al. (2000) showed the richness of mesoscale eddy fields and the formation of coastal currents and mesoscale eddies associated with the meteorological forcing and bottom topography.

In southeastern Lake Superior east of Marquette, Michigan, a warm, surface water pool was often found in summer, indicating the lack of wind driven upwelling processes (Bennett 1978; Phillips 1978). The integrated phytoplankton samples within the top 20 m showed a minimum of phytoplankton biomass (Munawar and Munawar 1978). Contradictory to this minimum of phytoplankton biomass, zooplankton samples in the top 100 m showed that this area is a maxima in zooplankton abundance (Watson and Wilson 1978). Such mismatch, caused by behavior and advection, could exist on relatively small spatial scales (Bollens et al. 1992; Steele and

[1] Corresponding author (mzhou@d.umn.edu).

Acknowledgments

Authors thank Jean Captain and all crew on the R/V *Blue Heron* for their support.

This project is supported by the Grant-in-Aid fund to M.Z. from the University of Minnesota and the Olsen scholarship for Summer Undergraduate Research to S.P. from the Department of Physics, University of Minnesota at Duluth.

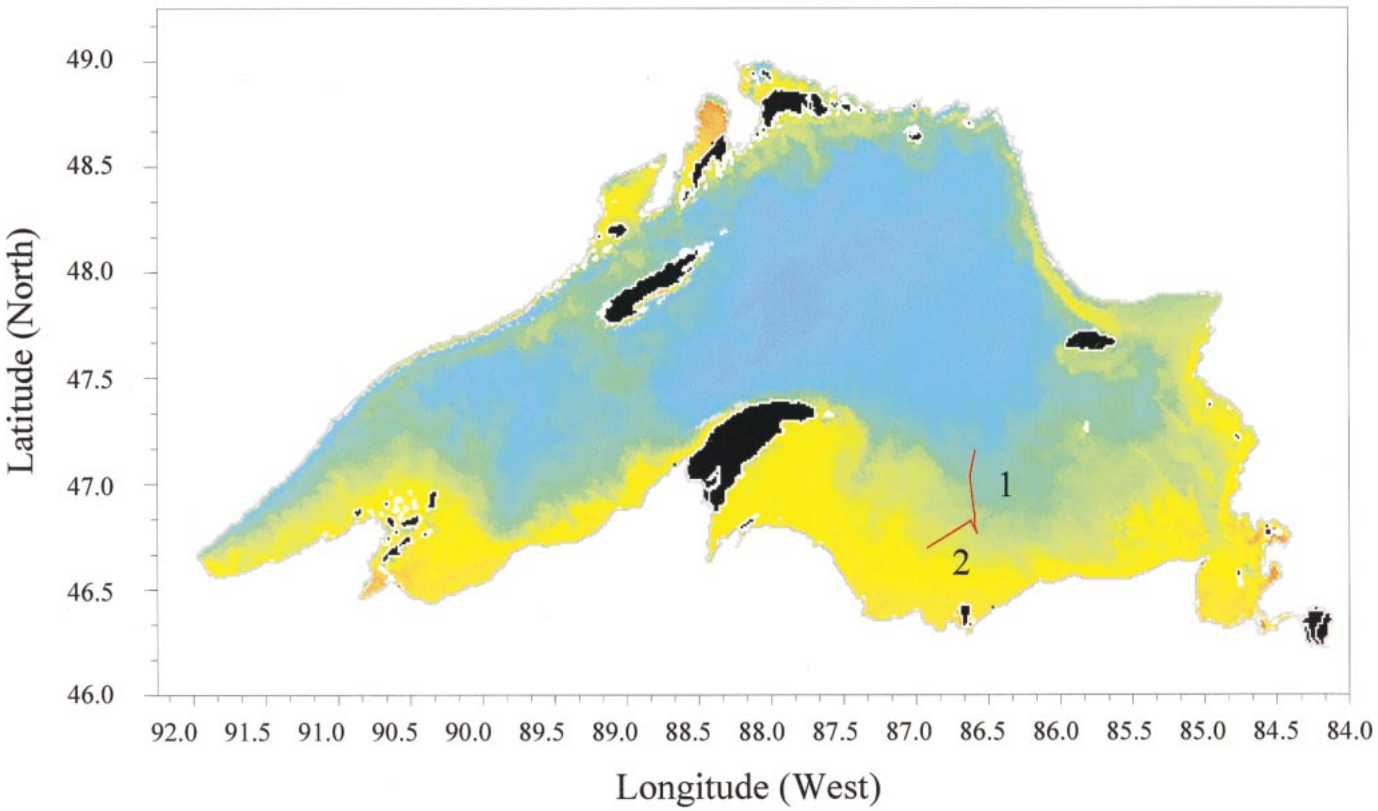

Fig. 1. A color image AVHRR SST of Lake Superior on 17 July 1999. The solid red line is the cruise track consisting of two transects labeled 1 and 2.

Henderson 1992). On a large scale, trophic energy transfer dictates the distribution.

What kinds of physical and biological processes lead to a high zooplankton abundance in southeastern Lake Superior? In this region there are rich mesoscale eddy features embedded in the coastal thermal front that can be easily recognized from the Advanced Very High Resolution Radiometer (AVHRR) Sea (Lake) Surface Temperature (SST) image (Fig. 1, courtesy of J. Budd, Michigan Technological University). At the latitude of Lake Superior (~47°N), the internal Rossby deformation radius is ~5–10 km (Pedlosky 1987). At this mesoscale, the thermocline can be tilted and lifted up to 10^0–10^1 m. The importance of mesoscale eddies to biological processes has been well documented in the Gulf Stream rings and in the California Current (Wiebe et al. 1992; Huntley et al. 1995; Zhou and Huntley 1997; Zhou 1998). These physical processes and their effects on biological processes, however, have not been well understood in the Great Lakes. In order to gain insights into these physical and biological processes, a cruise was conducted in southeastern Lake Superior to resolve both physical and biological fields at high resolutions.

Methods

The instruments used in this study include an SBE19 conductivity-temperature-depth (CTD; Sea-Bird Electronics) profiler, a Wetstar fluorometer (WET Labs), and an optical plankton counter (OPC; Focal Technologies). Technical details of the OPC can be found in Herman (1992) and Herman et al. (1993). In order to have high-resolution measurements both vertically and horizontally, we designed a simple towing frame that can vertically undulate while the ship steams at 3–4 knots. This towing frame was designed to be a simple vehicle providing the mounting space and protection for desired instruments towed through the water column. The frame can handle a maximum towing speed of 4 knots and maintains a stable flight path between the surface and 200 m. A hydraulic winch was used for controlling the depth by changing the wire length. During our survey the towed instrument package undulated between the surface (<2 m) and a depth of 100 m in a period of ~8 min cycle^{-1} at a towing speed of 3 knots.

The conducting wires in the towing cable provided simultaneous communication between the instruments and a data acquisition computer located in the ship's dry lab. CTD and fluorometer measurements were sent to the OPC through two jumper cables. The OPC integrated data from all three instruments into one data string and sent this information to the data acquisition computer in real time. GPS information was acquired through a serial communication port on the data acquisition computer and was also integrated into the OPC data strings.

The cruise was carried out from 15 to 20 July 1999 on-

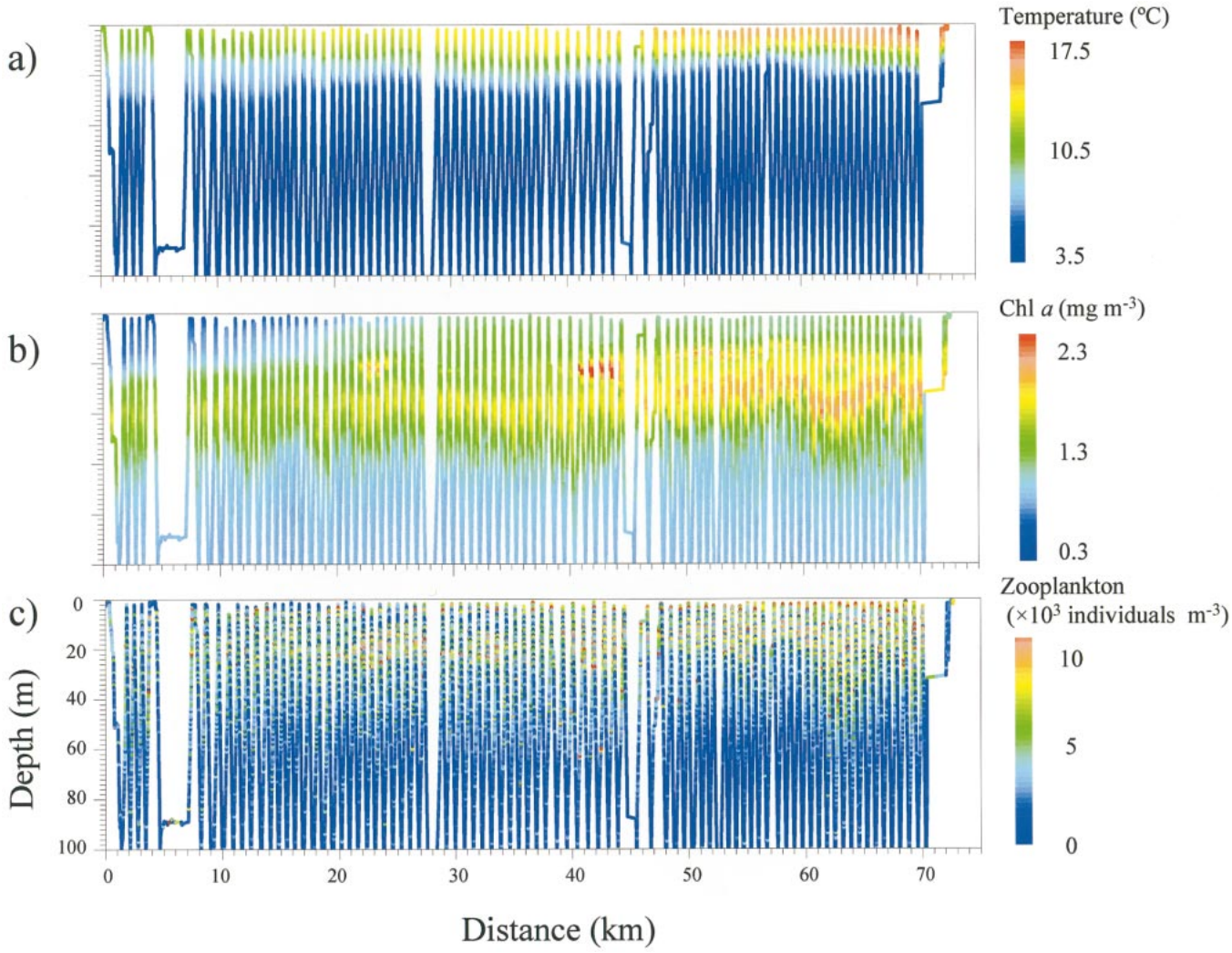

Fig. 2. The raw data binned into 1-m vertical intervals along the trajectory of the towed instrument package: (a) temperature, (b) chl *a*, and (c) zooplankton abundance. NOTE: Horizontal distance (km) is from the beginning to the end of both transects, putting the 0-km mark farthest offshore and 70 km nearest to shore.

board the R/V *Blue Heron*. Our measurements were taken along the transect illustrated in Fig. 1. To avoid any bias produced by diel vertical migration behavior of zooplankton, most of the measurements were taken on 17 and 18 July 1999 between dusk and dawn. The first deployment started at ~1700 h on 17 July from 47.25°N, 86.6°W near the deepest depth of Lake Superior. The transect continued due south for ~45 km and ended at ~0100 h on 18 July at 46.75°N, 86.6°W. The second deployment started near the end of the first transect at ~2100 h on 18 July, heading due southwest, and ended at ~0600 h on 19 July at 46.7°N, 87.1°W.

Data

The high-resolution OPC measurements, both vertically and horizontally, provide a basis for studying spatial variability of size-structured zooplankton populations. The OPC uses optical sensors to measure the equivalent spherical diameter (ESD) of particles passing through the flow-through tunnel. A particle with a size range from 250 μm to 14 mm is classified into one of 3,494 digital size classes.

Raw OPC data, based on one measurement per particle, were integrated into 40 body size increments on an equal $\log_{10}$ basis from 250 μm to 14 mm and normalized by both the interval of body size and the volume filtered through the aperture at 1-m vertical intervals. The abundance of zooplankton was then calculated by integrating all size categories. Averaging at 1-m intervals provides the highest resolution obtainable for temperature. In a 1-m interval, however, the water volume filtered by an OPC is approximately equal to 0.0066 m^3. If we assume that the abundance of zooplankton is on the order of 5×10^3 individuals m^{-3}, an OPC only measures 33 zooplankton per meter traveled, making it necessary to integrate the 3,494 size classes into fewer—in this case, 40. Even with this integration, undersampling occurred in all size classes, and the measurements showed a large variance (Fig. 2c).

Another obvious phenomenon shown in Fig. 2 is the mis-

match between up and down casts in CTD and fluorescence measurements. Such mismatch is caused by the delay of the instruments responding to the environment, which is a common problem encountered while using a rapidly undulating vehicle. Here the mismatch is approximately <2 m in the temperature profile and 5 m in the fluorescence profile.

The undersampling and mismatch can be further analyzed statistically by the method of objective analysis (Bretherton et al. 1976; Zhou 1998). In our calculation, we first calculated the variances of measurements. Second, the spatial correlation functions were obtained by computing the autocorrelation of each measurement. Then, the spatial interpolation was computed based on minimizing the least squares error, which leads to optimal interpolations (Fig. 3c).

One important component of currents in large lakes is the geostrophic current produced by the horizontal pressure gradient (Pedlosky 1987). The density field was directly obtained from the temperature field, and then the dynamic heights were further calculated. The geostrophic currents were calculated from the balance between the Coriolis force and the dynamic height. To solve this differential equation, we assume that the velocity is equal to zero at a depth of 100 dbar. Results of the geostrophic current calculation are shown in Fig. 3a.

Results and Discussion

Spatial scales in temperature and current fields—The temperature and geostrophic current fields showed strong spatial variability at both large and mesoscales (Fig. 3a). The lake temperature in the upper warm layer (0–10 m) changed from 9°C at the offshore area to <17°C at the nearshore area, which shows the warm water pool in the nearshore region. Throughout this 70-km transect, the thermocline varied in depth and width. At the beginning of the transect, the lower thermocline penetrated nearly 30 m into the water column. At ~60 km into the transect, the lower thermocline penetrated into only 20 m of the water column. In addition, the vertical temperature gradient was the least at the beginning of the transect and the greatest toward the end of the transect. Along this large-scale trend, the mesoscale (10–20 km) internal wave pattern in the thermocline becomes apparent and will be discussed later.

The geostrophic current penetrated down only 40 m. This result supports our assumption that there is no current at a depth of 100 m. The geostrophic current shows a complicated circulation pattern. The large-scale trend consists of the temperature gradient between warmer coastal surface water and cooler offshore water, leading to a general eastward coastal current. However, there were rich mesoscale activities superimposed on this large-scale trend, demonstrated by surface countercurrents at a scale of 10–20 km. There was a strong southeastward surface current up to 7 cm s^{-1} and a weak counter-undercurrent of ~1–2 cm s^{-1} below a depth of 20 m within 58–70 km into the transect. The location of this coastal current corresponded to the boundary of the nearshore warm water shown in the AVHRR SST image (Fig. 1). Offshore, there was a northwestward surface countercurrent up to 3 cm s^{-1} and then another eastward surface current up to 7 cm s^{-1}. Farther offshore, both temperature and currents showed relatively small-scale oscillations.

Relationship between the temperature and phytoplankton fields—The trends in chlorophyll *a* (chl *a*) distribution show a general decrease in concentration toward the offshore area (Fig. 3b) and maximum concentration beneath the thermocline (Fig. 4). In the upper 10 m, the concentration of fluorescence was ~1.2 mg m^{-3}. However, the concentration of chl *a* was extremely low (~0.5 mg m^{-3}) in the first 20 km of the deployment in the offshore area. Between the depths of 30 and 40 m (below the thermocline), chl *a* remained dominant throughout the transect with concentrations >2.0 mg m^{-3} in the nearshore area.

What caused the direct correlation between the chl *a* maximum in the vertical profile and the lower boundary of the thermocline? The distribution of mesozooplankton is relatively more patchy than chl *a*. Their grazing may produce holes in the chl *a* distribution, but they cannot produce the uniform correlation between the chl *a* maximum and the lower thermocline along this 70-km transect. Although microzooplankton may play a more important role in grazing chl *a* than mesozooplankton (Munawar et al. 1978), it is unlikely that microzooplankton would stop their grazing uniformly at the lower boundary of the thermocline. Grazing by micro- and mesozooplankton cannot explain the consistent correlation between the chl *a* maximum and the lower thermocline. Among the physical processes, if the chl *a* maximum in the vertical profile was produced by horizontal transport, the horizontal scale of the chl *a* distribution should be determined by the internal Rossby radius of 10–20 km, which is smaller than the observed scale of the large-scale trends in phytoplankton distribution. The chl *a* maximum was neither controlled by the vertical sinking of phytoplankton nor by their buoyancy because the maximum occurred in the deep water where the density is relatively uniform. Thus, we hypothesize that the biochemical environment of the deep water and the change of light field as a function of the depth lead to a correlation between the chl *a* maximum and the lower thermocline.

Photoinhibition could cause a surface minimum in the vertical distribution of chl *a*. The studies of photoinhibition in freshwater showed that the irradiance producing photoinhibition is ~120 W m^{-2} (Kirk 1983). The maximum photosynthetically available radiation (PAR) without cloud correction at the surface was approximately equal to 425 W m^{-2} during our survey period. Using a vertical extinction coefficient of 0.1–0.2 m^{-1} for this region, the depth of photoinhibition could reach only to 6–13 m (Schertzer et al. 1978). The surface minimum of chl *a* concentration in the offshore area penetrated to a depth of 20 m, which is much deeper than the depth of photoinhibition. This implies that the productivity in the surface water was limited by other biological and chemical factors instead of light.

The depth of the euphotic zone (z_e) can be estimated by the condition $I(z_e)/I_0 = 1\%$ (Kirk 1983). If we take the vertical extinction coefficient of 0.1–0.2 m^{-1}, the depth of the euphotic zone varies from 23 to 46 m (Schertzer et al. 1978). In our observations, the lower thermocline was uplifted from

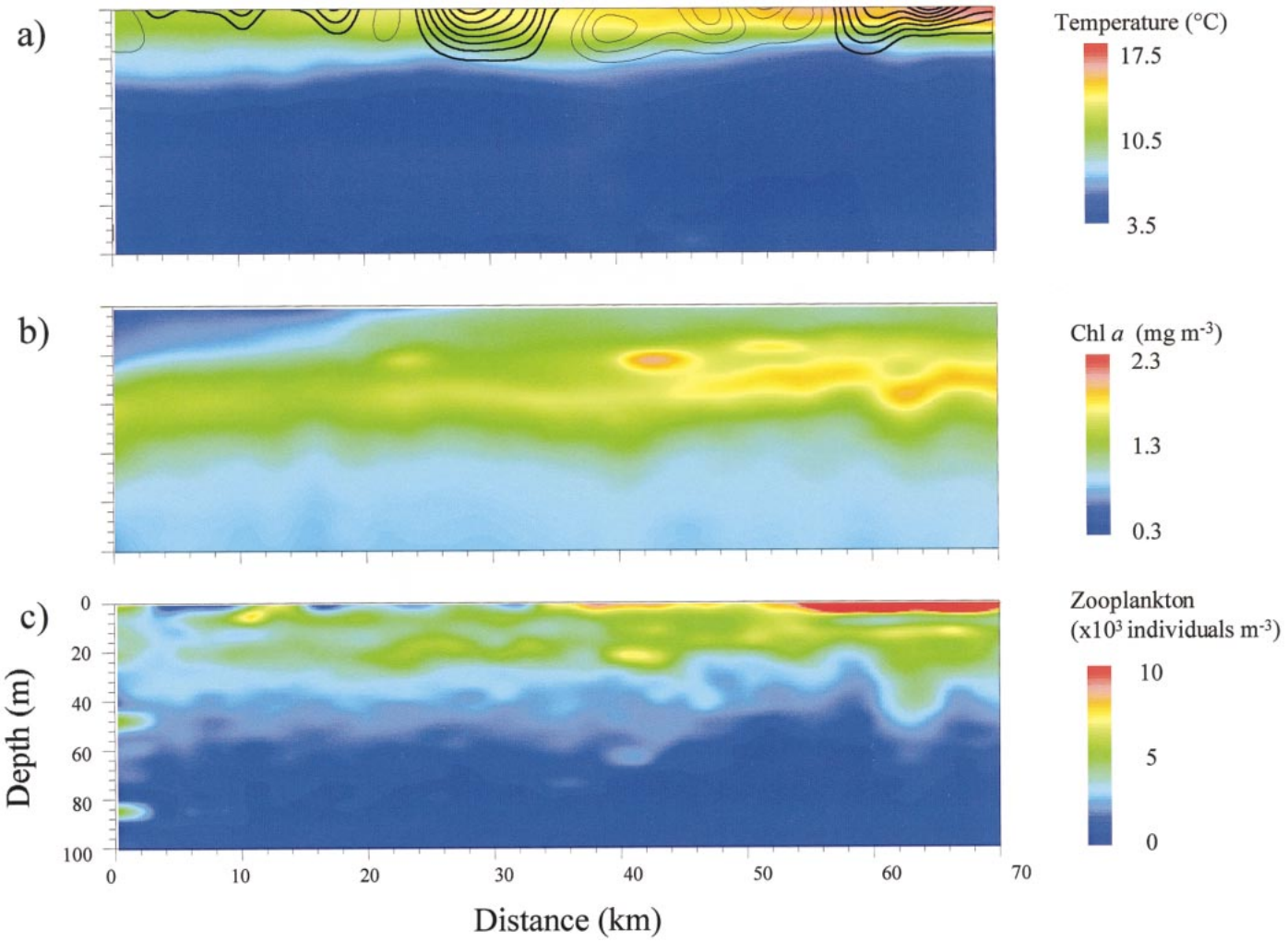

Fig. 3. The objectively interpolated results showing (a) the temperature (color image) and geostrophic current (contours), (b) chl *a*, and (c) zooplankton abundance. Solid contour lines start from 1 cm s^{-1} with 1 cm s^{-1} contour intervals. Dashed contour lines start from −1 cm s^{-1} with 1 cm s^{-1} contour intervals. The positive is toward the southeast or east. NOTE: Horizontal distance (km) is from the beginning to the end of both transects, putting the 0-km mark furthest offshore and 70 km nearest to shore.

30 m in the offshore area to 20 m in the nearshore area. The depth of the lower thermocline varied within the euphotic zone. If the primary productivity in the surface layer is limited by some biological and chemical factors, the occurrence of a chl *a* maxima in the deep water within the euphotic zone indicates that the deep water beneath the thermocline is more biologically productive than the surface water. Hence, the high productivity in the nearshore area may be directly associated with this uplifting of the thermocline, which allows higher productive deep water into the euphotic zone.

In addition to the positive correlation between the offshore–nearshore gradient of chl *a* below the thermocline and the large-scale tilting of the thermocline, the chl *a* concentration covaried with the mesoscale variation of the thermocline. This covariation can be produced by both the vertical movements of the thermocline and shifting in irradiance caused by the vertical motion. It is clear that the depth of the lower thermocline may determine the location and degree of primary production.

In the horizontal chl *a* distribution, the offshore surface minimum distinguishes the surface water of the central gyre from the nearshore water. The survey indicates that the concentration of chl *a* in the surface water within the first 10 km is even less than the ambient chl *a* in the deep water and nearshore water, which further proves that the chl *a* maximum beneath the thermocline is independent of the productivity in the surface water.

Relation between temperature, phytoplankton, and zooplankton fields—The abundance of zooplankton was the greatest (up to 10×10^3 individuals m^{-3}) in the upper 10 m of the nearshore water column, where the water was the warmest, and decreased offshore (Fig. 3). In the vertical, there were two layers of zooplankton, one right at the surface and the other at the thermocline. This two-layer phenomenon

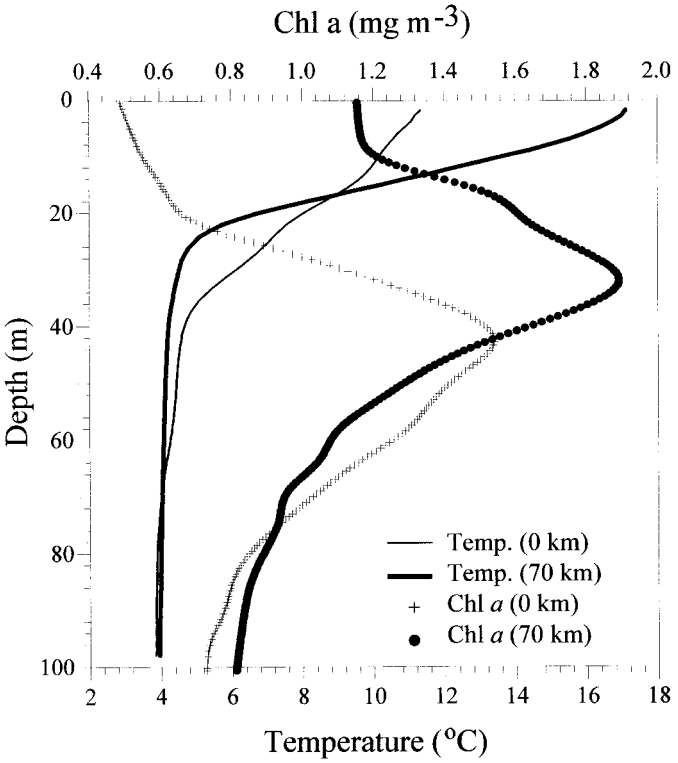

Fig. 4. The vertical profiles of temperature and chl *a* at 0 and 70 km.

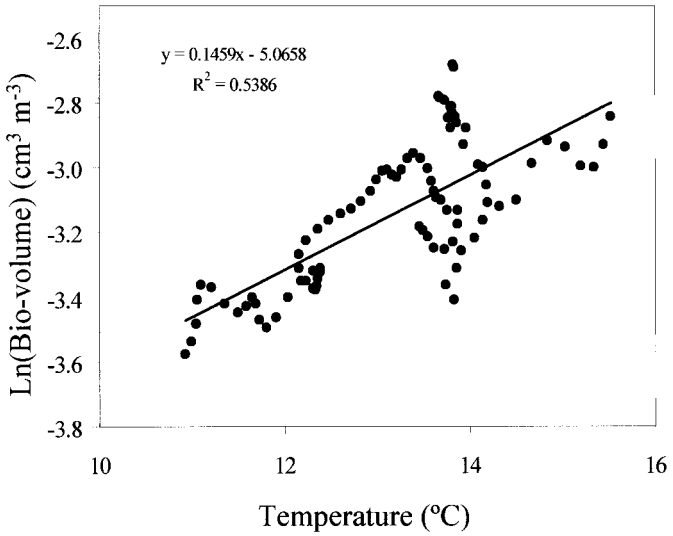

Fig. 5. The relation between the average temperature and biovolume of zooplankton in the upper 10 m.

was also found in acoustic measurements made in the western arm of Lake Superior (Megard et al. 1997). All our measurements were made at night, and all acoustic measurements were made during the day, suggesting that such a two-layer feature is a constant phenomenon regardless of day and night. Zooplankton abundance decreased to zero below a depth of 60 m.

Previous studies in Lake Superior suggested that the zooplankton biomass was directly proportional to the water temperature and exposure time (Watson and Wilson 1978). The regression of zooplankton biomass and temperature in the top 10 m showed an exponential relation

$$B \sim e^{\alpha T}, \tag{1}$$

where T is the temperature in °C, B is the total zooplankton biomass, and α is the exponent, which is equal to 0.136 converted from the value at the $\log_{10}$ basis in Watson and Wilson (1978). We plot the temperature versus ln(zooplankton biovolume), which are averaged in the upper 10 m (Fig. 5). The conversion from biovolume to biomass may affect the intercept but should not affect the slope (i.e., the exponent in Eq. 1). Our regression showed that the exponent α is equal to 0.146 with r^2 0.54. This result is not significantly different from the results of previous studies, but the confidence is lower. Without averaging the temperature and zooplankton biovolume, the correlation between the biomass and the temperature is even lower ($r^2 < 0.1$). We should point out that the correlation between the biomass and temperature obtained from Watson and Wilson (1978) is primarily driven by the seasonal change instead of the spatial variability; thus, we cannot extrapolate Eq. 1 in the spatial interpolation.

The relation between the temperature, fluorescence, and zooplankton abundance is also explored by plotting the temperature versus fluorescence with color codes representing the abundance of zooplankton (Fig. 6). Most of our data below the thermocline are concentrated near 4°C at low chl *a* concentrations <1 mg m^{-3} and low zooplankton abundance $<2 \times 10^3$ individuals m^{-3}. Although high chl *a* concentrations were found between 4 and 4.5°C, there were only small amounts of zooplankton in this temperature region. Zooplankton were abundant in the region of 5–17°C with relatively high chl *a*, where the upper envelope shows an inverse relation between chl *a* and temperature in the nearshore area. In the highest temperature region (15–17°C), there are high abundances of zooplankton, even though the chl *a* is only one-half of the value in the region of 4–4.5°C. The envelope of the measurements at the lowest chl *a* level represents the offshore surface water with low zooplankton abundances. It appears that zooplankton tended to avoid the water near 4°C and were widely spread throughout a large range of both temperature and fluorescence.

Size-structured zooplankton populations—The design of the OPC is such that it should be capable of detecting particles between 250 μm and 14 mm in ESD, although some recent studies suspect the detection capability may extend down to 150 μm for certain species (Herman pers. comm.). Based on a previous study, the majority of Lake Superior zooplankton appear to be between 300 and 1,500 μm in length, although Watson and Wilson (1978) used a fine mesh net (64 μm), which might not be effective in catching larger zooplankton. Taxonomic keys for Lake Superior (Balcer et al. 1984) indicate that only a few, uncommon cladoceran species may exceed the 14-mm detection capability of the OPC.

It is a difficult task to correlate OPC data (reported as ESD) and actual genera of zooplankton because an OPC does not provide any information on the body shape. Be-

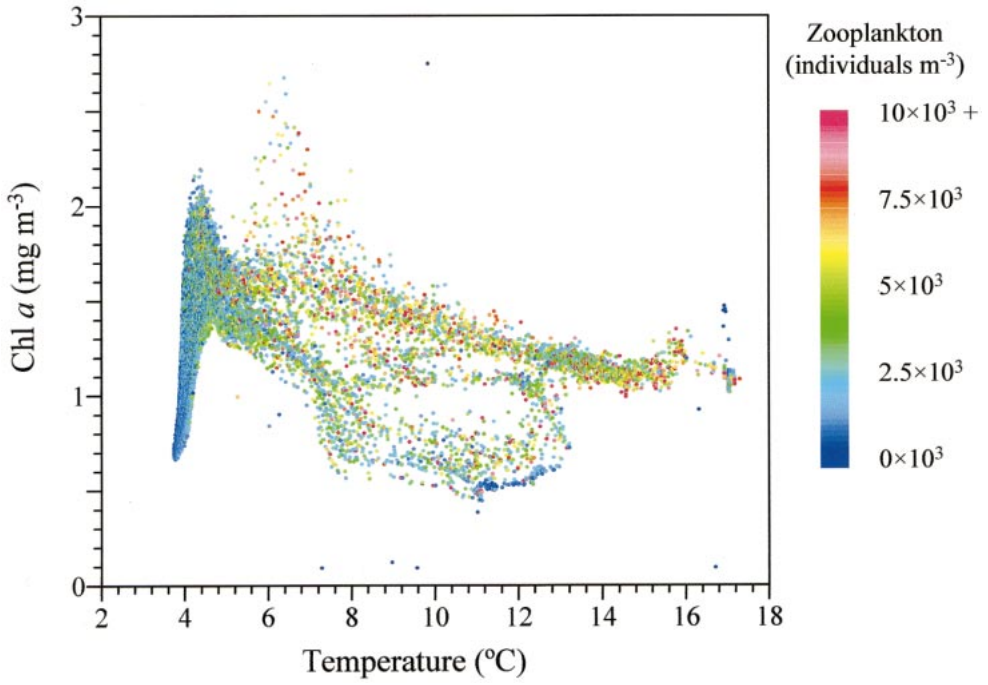

Fig. 6. The scatter plot of the temperature versus chl *a*, with color codes representing zooplankton abundance.

cause body shape varies greatly among zooplankton, many problems persist relating ESD to actual body volume. A recent report by Sprules et al. (1998) provides additional information regarding the precision of OPC measurements in freshwater systems, noting that errors are minimized at zooplankton abundances $<30 \times 10^3$ individuals m^{-3}. In our measurements, the maximum abundance is approximately equal to 10×10^3 individuals m^{-3}. Table 1 provides historical estimates of the zooplankton composition in Lake Superior with average body length and ESD approximations for the more common species.

Results of our survey agree with the heterogeneous distribution implied by Watson and Wilson (1978) in that there is an onshore and offshore variation in zooplankton distri-

Table 1. The dominant zooplankton of Lake Superior as classified by percentage of total numbers (Watson and Wilson 1978). Length and width estimates were interpolated from Balcer et al. (1984).

	% total numbers	Length (mm)	L : W ratio	Av. ESD (μm)
Calanoid copepods				
Diaptomus sicilis (adult)	11	1.5–1.8	3.3 : 1	920–1,105*
Diaptomus ashlandi (adult)	2.5	0.9–1.1	3.3 : 1	550–675
Diaptomus spp. (copepodite)	18	0.4–1.3	3.3 : 1	250–800
Diaptomus spp. (nauplii)	44	0.3	2.5 : 1	184
Limnocalanus macrurus	5.5	2.4–2.9	3.2 : 1	1,475–1,780
Senecella calanoides	0.6	2.6–3.3	3.2 : 1	1,600–2,025
Calanoid total	81.6			
Cyclopoid copepods				
Cyclops bicuspidatus thomasi (adult)	1	1.0–1.4	3 : 1	615–860
Cyclops spp. (copepodite)	6.5	0.3–0.8	3 : 1	185–490
Cyclops spp. (nauplii)	5	0.15	2.5 : 1	92
Cyclopoid total	12.5			
Cladocerans				
Bosmina longirostris	1.2	0.4–0.6	1.2 : 1	245–370
Daphnia galeata mendotae	3	1.5–2.0	1.7 : 1	920–1,230*
Holopedium gibberum	0.2	1.0–1.7	1.2 : 1	615–1,040
Cladoceran total	4.4			
Total	98.5			

* Sprules et al. (1998) made direct measurements on *Diaptomus leptopus* and *Daphnia magna* using an OPC. Results over a similar size range showed an average ESD of ~1,250 and 1,400 μm, respectively.

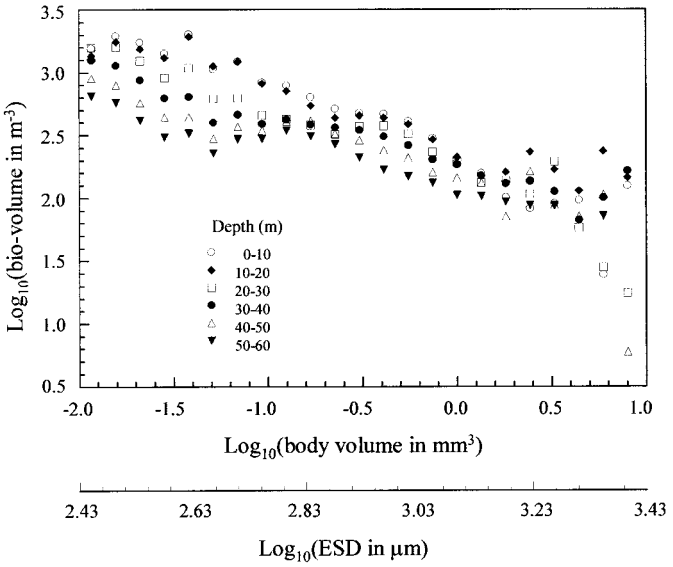

Fig. 7. Horizontally averaged biovolume spectra between 0 and 10 m, 10 and 20 m, 20 and 30 m, 30 and 40 m, 40 and 50 m, and 50 and 60 m deep.

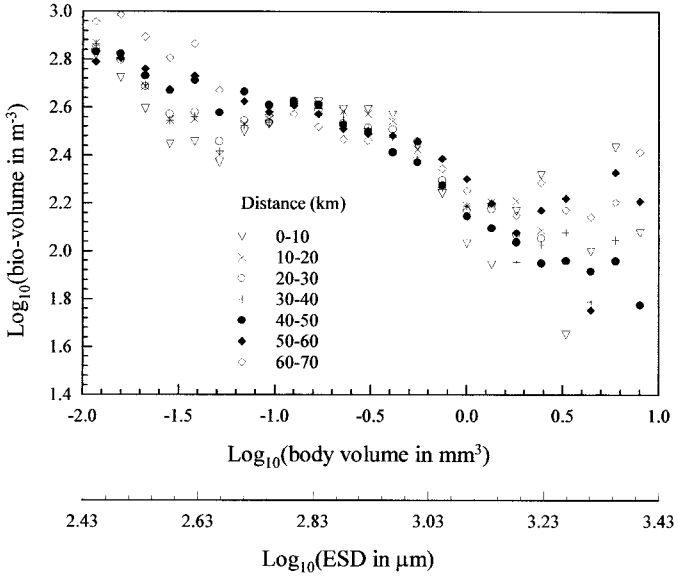

Fig. 8. Vertically averaged biovolume spectra (0–60 m) at 0–10 km, 10–20 km, 20–30 km, 30–40 km, 40–50 km, 50–60 km, and 60–70 km.

bution. Figure 7 shows the biovolume spectra in 10-km horizontal bins vertically averaged between the surface and 100 m. The distance 0 is at the beginning of the first transect. The biovolume spectra in Fig. 7 shows three different trends associated with horizontal distance and body volume. Biovolume shows a distinctive dome between body volumes of 0.05 and 0.6 mm^3 in the offshore area (0–40 km). We suspect the dome is associated with some offshore zooplankton species. The number of zooplankton counted in this body volume range is ~14% of the total counts. Assuming a body length–width ratio of 3:1, the equivalent body length range for the dome is ~0.8–2 mm. Comparing this to data from Watson and Wilson (1978), two of the dominant zooplankton they found in Lake Superior fit into this body length range: *Diaptomus sicilis* and *D. ashlandi* adults. These two species made up 14% of the total zooplankton composition in the Watson and Wilson (1978) data as well. Because we didn't collect net samples during our OPC tows, we cannot say if the match of the results is purely coincidence or an indication that the OPC could be used to identify distinct species.

Figure 8 shows the biovolume spectra in vertical 10-m bins horizontally averaged over the second transect. The biovolume spectra on body volumes larger than 10 mm are not shown because of undersampling. The spectra are averaged in every 10-m depth interval, providing a vertical distribution of the zooplankton size structure. The biovolumes in the top 20 m have the highest concentrations, and biovolume spectra are almost homogeneous in the individual body volume range from 0.01 to 1 mm^3. From 20 m deep and below, the biovolume decreased with depth throughout the individual body volume range from 0.01 to 1 mm^3. The slopes of the biovolume spectra get flatter with increasing depth, indicating that the change of size structure in the upper water column is more profound than at depth.

The slope of a biovolume spectrum can be interpreted in terms of population dynamics rates (Heath 1995; Zhou and Huntley 1997). In order to compare with other studies in different regions, we converted a biovolume spectrum to a biomass spectrum using the relationship between body length and body carbon obtained by Rodríguez and Mullin (1986). Although the accuracy of this relation is questionable for freshwater zooplankton, it should be justified in the first-order approximation. In Fig. 9, we composed several biomass spectra from different regions around the world. The biomass spectra in the California Current and Ross Sea regions were averaged between the surface and a depth of ~300 m (Zhou and Huntley 1997; Zhu et al. 1998). The biomass spectrum at the JGOFS Hawaii Ocean Time-series (HOTS) station in the subtropic Pacific was calculated in the mixed layer between 25 and 35 m (Zhou, unpubl. data). The biomass spectrum in the Norwegian fjords was averaged between the surface and 5 m above the bottom, which varied from 25 to 150 m (Edvardsen pers. comm.). The averaged biomass spectrum in Lake Superior was obtained between the surface and bottom (Sprules and Munawar 1986), and for this study, over the whole transect between the surface and 100 m. Comparing those various spectra, the first surprising result is that the zooplankton biomass for Lake Superior is equivalent to or higher than those of the most biologically active regions, such as the California Current and the Norwegian fjords, and higher than the historic values of Lake Superior, especially for large sizes of zooplankton.

If we take the mean temperature of ~12°C in the mixed layer, the optimal time scale for a zooplankter to double its weight is ~6 d (Huntley and Lopez 1992). Compared with the seasonal time scale of 30–60 d, the time scale of zooplankton growth is relatively small. Thus, the spatially averaged biomass spectrum can be assumed to be at quasi–steady state. The slope of the biomass spectrum represents the ratio of specific population mortality to specific individual body mass growth rates (Zhou and Huntley 1997). This slope is nearly a constant of approximately −0.7 in the body

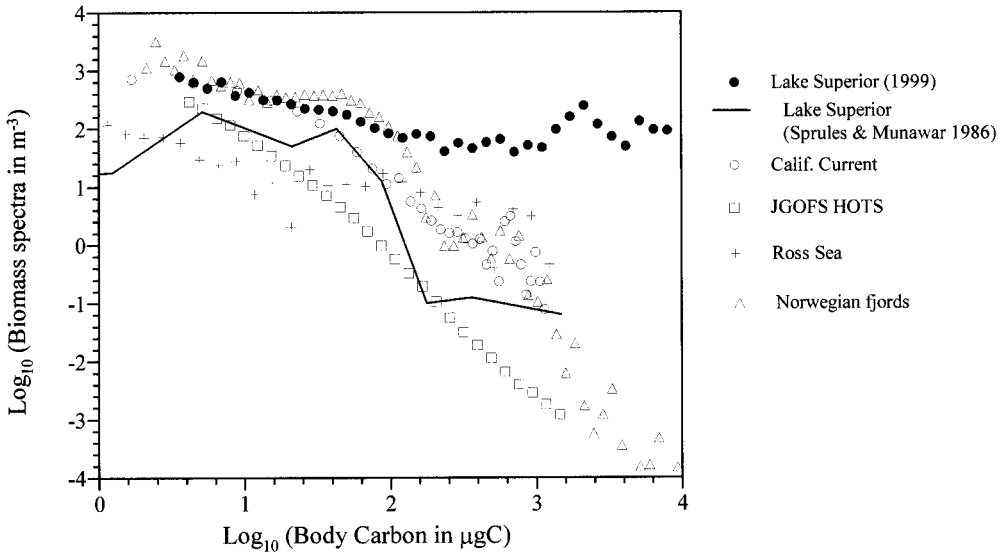

Fig. 9. Biomass spectra from various regions of the world. The biomass spectra in the California Current and Ross Sea regions were averaged between the surface and a depth of ~300 m (Zhou and Huntley 1997; Zhu et al. 1998). The biomass spectrum at the JGOFS HOTS station in the subtropical Pacific was calculated in the mixed layer between 25 and 35 m (Zhou, unpubl. data). The biomass spectrum in the Norwegian fjords was averaged between the surface and 5 m above the bottom, which varied from 25 to 150 m (Edvardsen pers. comm.). The averaged biomass spectrum in Lake Superior was obtained between the surface and bottom (Sprules and Munawar 1986) and, for this study, over the whole transect between the surface and 100 m.

weight range up to $\sim 10^3$ μg C and fluctuates with a mean slope nearly equal to zero in the larger size classes. The second surprising result is that the absolute value of the slope, the absolute ratio of specific mortality to specific individual growth rates, is much smaller than those of other regions, and the historic value for Lake Superior (approximately -1.3) (Sprules and Munawar 1986).

A flatter slope indicates faster individual growth and lower mortality. If we assume that zooplankton growth is dictated by the temperature and is not limited by available food, the mortality in Lake Superior is two times smaller than that of other regions. With the consideration of food limitation, the mortality could even be less. Many hypotheses can be made to explain the low mortality in Lake Superior, such as the reduction of planktivorous fish through overfishing or an adopted fast growth of zooplankton in the warm surface water while their predators maintained a low metabolism in cold water. We are not able to give definite answers by our limited data. However, it is certain that there is a large zooplankton pool with very low mortality in Lake Superior, which needs to be supported by lower trophic-level biomass.

Summary: A physical process forced system—The current system showed complicated coastal and countercurrents, which indicates the nature of rich mesoscale eddies in Lake Superior. Eddies and meanders superimposed on the coastal fronts can easily be identified from the AVHRR SST image (Fig. 1). However, the tilting of the thermocline cannot be easily interpreted from the surface temperature. A subthermocline maximum cannot be detected by satellite remote sensing because the depth of the maximum is beneath the optical detection depth.

Occurrence of the subthermocline maximum of chl *a* suggests that the deep water in Lake Superior is more biologically productive than the surface water. The variation of this maximum may directly respond to the depth change of the lower boundary of the thermocline. In previous work, most of the phytoplankton samples were taken by nets in the upper 10 m with bottle samples taken at 5, 10, 25, and 50 m (Munawar and Munawar 1978). However, our measurements showed that the subthermocline maximum of chl *a* occurred around a depth of 30–40 m.

The warm surface water and available food in the subsurface cold water provided the necessary conditions for zooplankton to feed and grow. Both phytoplankton and zooplankton covaried with each other at the large scale and decreased in concentration and abundance toward the offshore area. The vertical distribution of chl *a* and zooplankton, however, was negatively correlated.

The abundance of zooplankton reached 10×10^3 individuals m^{-3} in the warm surface water and was down to 3×10^3 individuals m^{-3} at 40–50 m. Although most of the zooplankton remained in the surface waters, a second layer of zooplankton occurred at the 10–20-m depth interval, where they might actively feed on the upper portion of the phytoplankton layer.

References

BALCER, M. D., N. L. KORDA, AND S. I. DODSON. 1984. Zooplankton of the Great Lakes: A guide to the identification and ecology of the common crustacean species. Univ. of Wisconsin Press.

BENNETT, E. B. 1978. Characteristics of the thermal regime of Lake Superior. J. Great Lakes Res. **4:** 310–319.

BOLLENS, S. M., B. W. FROST, H. R. SCHWANINGER, C. S. DAVIS, K. J. WAY, AND M. C. LANDSTEINER. 1992. Seasonal plankton cycles in a temperate fjord and comments on the match–mismatch hypothesis. J. Plankton Res. **14:** 1279–1305.

BRETHERTON, F. P., R. E. DAVIS, AND C. B. FANDRY. 1976. A technique for objective analysis and design of oceanographic experiments applied to MODE-73. Deep Sea Res. **23:** 559–582.

CHEN, C., J. ZHU, E. A. RALPH, S. A. GREEN, AND J. BUDD. 2000. Prognostic modeling studies of the Keweenaw current in Lake Superior. Part I: Formation and evolution. J. Phys. Oceanogr. In press.

EL-SHAARAWI, A., AND M. MUNAWAR. 1978. Statistical evolution of the relationships between phytoplankton biomass, chlorophyll *a,* and primary production in Lake Superior. J. Great Lakes Res. **4:** 443–455.

FAHNENSTIEL, G. L., C. L. SCHELSKE, AND M. J. MCCORMICK. 1990. Phytoplankton photosynthesis and biomass in Lake Superior: Effect of nutrient enrichment. Int. Ver. Theor. Angew. Limnol. **24:** 371–377.

HEATH, M. R. 1995. Size spectrum dynamics and the planktonic ecosystem of Loch Linnhe. ICES J. Mar. Sci. **52:** 627–642.

HERMAN, A. W. 1992. Design and calibration of a new optical plankton counter capable of sizing small zooplankton. Deep Sea Res. **39:** 395–415.

———, N. A. COCHRANE, AND D. D. SAMEOTO. 1993. Detection and abundance estimation of euphausiids using an optical plankton counter. Mar. Ecol. Prog. Ser. **94:** 165–173.

HUNTLEY, M. E., AND M. D. G. LOPEZ. 1992. Temperature-dependent production of marine copepods: A global synthesis. Am. Nat. **140:** 201–242.

———, M. ZHOU, AND W. NORDHAUSEN. 1995. Mesoscale distribution of zooplankton in the California Current in late spring, observed by optical plankton counter. J. Mar. Res. **53:** 647–674,

KIRK, J. T. O. 1983. Light and photosynthesis in aquatic ecosystems. Cambridge Univ. Press.

LAM, D. C. L. 1978. Simulation of water circulation and chloride transport in Lake Superior for summer 1973. J. Great Lakes Res. **4:** 343–349.

MATHESON, D. H. AND M. MUNAWAR. 1978. Lake Superior basin and its development. J. Great Lakes Res. **4:** 249–263.

MEGARD, R. O., M. M. KUNS, M. C. WHITESIDE, AND J. A. DOWNING. 1997. Spatial distributions of zooplankton during coastal upwelling in western Lake Superior. Limnol. Oceanogr. **42:** 827–840.

MUNAWAR, M., AND I. MUNAWAR. 1978. Phytoplankton of Lake Superior 1973. J. Great Lakes Res. **4:** 415–442.

———, ———, L. R. CULP, AND G. DUPUIS. 1978. Relative importance of nannoplankton in Lake Superior phytoplankton biomass and community metabolism. J. Great Lakes Res. **4:** 462–480.

NALEWAJKO, C., AND K. LEE. 1981. Phosphorous kinetics in Lake Superior: Light intensity and phosphate uptake in algae. Can. J. Fish. Aquat. Sci. **38:** 224–232.

OLSON, T. A. 1969. A Study of the open water distribution and abundance of net plankton as an index of eutrophication in Lake Superior. OWRR Project No A-011-Mnn, Univ. of Minnesota.

PATALAS, K. 1972. Crustacean plankton and the eutrophication of St. Lawrence Great Lakes. J. Fish. Res. Board Can. **29:** 1451–1462.

PEDLOSKY, J. 1987. Geophysical fluid dynamics. Springer-Verlag.

PHILLIPS, D. W. 1978. Environmental climatology of Lake Superior. J. Great Lakes Res. **4:** 288–309.

RODRÍQUEZ, J., AND M. M. MULLIN. 1986. Relation between biomass and body weight of plankton in a steady state oceanic ecosystem. Limnol. Oceangr. **31:** 361–370.

ROSE, C., AND R. P. AXLER. 1998 Uses of alkaline phosphatase activity in evaluating phytoplankton community phosphorus deficiency. Hydrobiol. **361:** 145–156.

SCHERTZER, W. M., F. C. ELDER, AND J. JEROME. 1978. Water transparency of Lake Superior in 1973. J. Great Lakes Res. **4:** 350–358.

SPRULES, W. G., AND M. MUNAWAR. 1986. Plankton size spectra in relation to ecosystem productivity, size, and perturbation. Can. J. Fish. Aquat. Sci. **43:** 1789–1794.

———, E. H. JIN, A. W. HERMAN, AND J. D. STOCKWELL. 1998. Calibration of an optical plankton counter for use in fresh water. Limnol. Oceanogr. **43:** 726–733.

STEELE, J. H., AND E. W. HENDERSON. 1992. A simple model for plankton patchiness. J. Plankton Res. **14:** 1397–1403.

SWAIN, W. R., R. W. MAGNUSON, J. D. JOHNSON, T. A. OLSON, AND T. O. ODLAUG. 1970. Vertical migration of zooplankton in western Lake Superior, p. 619–639. *In* 13th Conf. of Great Lakes Research. International Association of Great Lakes Research.

WATSON, N. H. F., AND J. B. WILSON. 1978. Crustacean zooplankton of Lake Superior. J. Great Lakes Res. **4:** 481–496.

WEILER, R. R. 1978. Chemistry of Lake Superior. J. Great Lakes Res. **4:** 370–385.

WIEBE, P. H., N. J. COPLEY, AND S. H. BOYD. 1992. Coarse-scale horizontal patchiness and vertical migration of zooplankton in Gulf Stream warm-core ring 82-H. Deep Sea Res. **39:** S247–S278.

ZHOU, M. 1998. An objective interpolation method for spatiotemporal distribution of marine plankton. Mar. Ecol. Prog. Ser. **174:** 197–206.

———, AND M. E. HUNTLEY. 1997. Population dynamics theory of plankton based on biomass spectra. Mar. Ecol. Prog. Ser. **159:** 61–73.

ZHU, J., C. CHEN, E. A. RALPH, AND S. A. GREEN. 2000. Prognostic modeling studies of the Keweenaw current in Lake Superior. Part II: Simulation. J. Phys. Oceanogr. In press.

ZHU, Y., M. ZHOU, W. NORDHAUSEN, A. GONZALEZ, S. PINCA, X. ZHONG, AND M. E. HUNTLEY. 1998. Temporal and spatial variability of carbon flux contributed by meso-zooplankton in the Polar Front and Ross Sea, Antarctica. EOS **79:** 182–182.

Received: 28 January 2000
Accepted: 2 January 2001
Amended: 26 January 2001